

Research Article

Systematic Evaluation and Mechanistic Investigation of Antioxidant Activity of Fullerenols Using β -Carotene Bleaching Assay

Hiroshi Ueno, Shizuka Yamakura, Riya S. Arastoo, Takumi Oshima, and Ken Kokubo

Division of Applied Chemistry, Graduate School of Engineering, Osaka University, 2-1 Yamadaoka, Suita, Osaka Prefecture 565-0871, Japan

Correspondence should be addressed to Ken Kokubo; kokubo@chem.eng.osaka-u.ac.jp

Received 27 June 2014; Accepted 12 August 2014; Published 28 August 2014

Academic Editor: Naoki Kishi

Copyright © 2014 Hiroshi Ueno et al. This is an open access article distributed under the Creative Commons Attribution License, which permits unrestricted use, distribution, and reproduction in any medium, provided the original work is properly cited.

Antioxidant activity of hydroxylated fullerenes, so-called fullerenols, against lipid peroxy radical was evaluated by β -carotene bleaching assay. All samples showed moderate to high antioxidant activity (%AOA), especially for $C_{60}(OH)_{12}$ (70.1) and $C_{60}(OH)_{44}$ (66.0) as compared with 8, 24, 26, and 36 hydroxylated ones (31.7–62.8). The detection of the possible products was conducted in the model reaction of both fullerenols and C_{60} with methyl linoleate by MALDI-TOF-MS. These results suggested that the two possible mechanisms, such as C-addition to double bonds and H-abstraction from –OH groups, are involved in the present radical scavenging reaction.

1. Introduction

Fullerene known as “radical sponge” has been recognized as a new class of antioxidant due to its high reactivity toward radical species since its first report in 1991 [1]. Reactive oxygen species (ROS), such as superoxide, hydroxyl radical, peroxy radicals, and nitric oxide, have such radical nature and cause damage to biomolecules, including DNA, cell, protein, and lipid, inducing various diseases. For this reason, the development of biocompatible, nontoxic, and water-soluble fullerene derivatives has been strongly demanded. In the past several years, we have evaluated the ROS radical scavenging ability as “antioxidant activity” of water-soluble γ -cyclodextrin- (CD-) capped C_{60} and polyvinylpyrrolidone- (PVP-) entrapped C_{60} as well as the corresponding fullerene oxides ($C_{60}O_n$) [2, 3]. However, their solubility in water still remains low and inevitable steric repulsion from the host compounds, such as CD and PVP, brings about undesirable interference for accurate bioassay.

Polyhydroxylated fullerenes, so-called fullerenols, have attracted much attention in view of biological, pharmaceutical, and medical applications, because of their high hydrophilicity and the low toxicity as well as the unique

spherical structure with a diameter of ca. 1 nm. In this point of view, the antioxidant activity of fullereneol has been reported in 1995 by Chiang et al. for $C_{60}(OH)_{12}$ [4] and in 2009 by Miwa et al. for highly hydroxylated fullereneol $C_{60}(OH)_{32}$ [5] as well as other bioactivities, such as the inhibitive effect for oxidative stress in adipocytes [6], protective effect of human keratinocytes from UV-induced cell injuries [7], and suppression of intracellular lipid accumulation [8]. In connection with the recent developments of these biological studies [9–11], new and facile synthetic procedures of highly hydroxylated water-soluble fullerenols have been reported [12–14]. However, little is known about their origin of antioxidant activity and the relationship between the activity and the number of hydroxyl groups. For the development of new application of these unique nanomaterials, the systematic investigation of the antioxidant activity of variously hydroxylated fullerenols, such as 8, 10, 12, 24, 26, 36, and 44 hydroxylated ones [15], is highly desirable to explore the antioxidant mechanism of fullerenols toward ROS (Figure 1).

The β -carotene bleaching assay for evaluating antioxidant activity is one of the common methods used in the field of food chemistry [16]. The principle of the method is based on the discoloration of yellowish color of a β -carotene solution

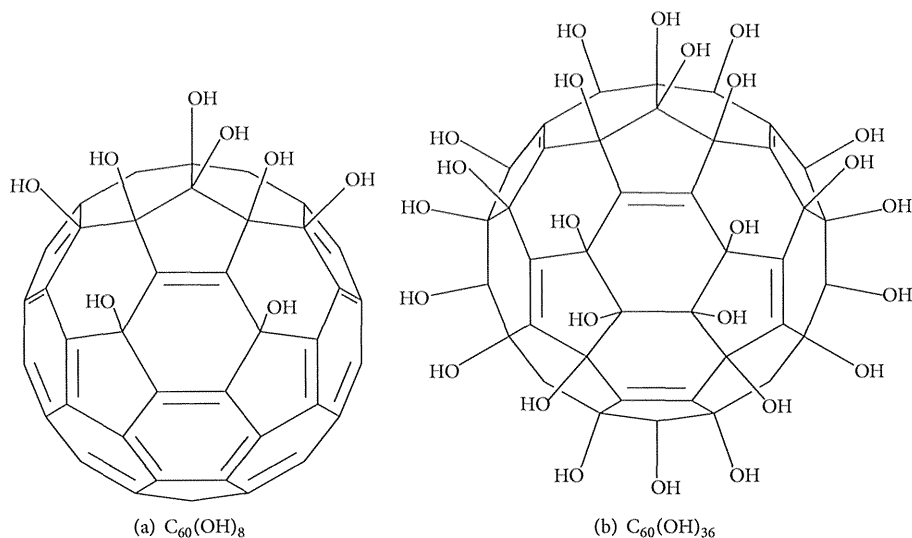


FIGURE 1: A possible isomer of fullerlenols composed of a mixture of isomers and expressed by the average structures as (a) $C_{60}(OH)_8$ and (b) $C_{60}(OH)_{36}$.

due to the breaking of π -conjugation by addition reaction of lipid or lipid peroxyl radical (L^* or LOO^*) to a C=C double bond of β -carotene. The radical species is generated from the autoxidation of linoleic acid by heating under air atmosphere. When the appropriate antioxidant is added to the solution, the discoloration can be retarded by competing reaction between β -carotene and antioxidant with the subjected radicals. The structural similarity between fullerenes and β -carotene, such as highly π -conjugated molecules, enables the accurate evaluation of antioxidant activity by this β -carotene bleaching assay in contrast to other methods like DPPH radical assay [17].

Herein, we report the systematic investigation of antioxidant activity of variously hydroxylated fullerlenols with 8, 10, 12, 24, 26, 36, and 44 hydroxyl groups evaluated by β -carotene bleaching assay. In combination with detecting the possible products of both fullerlenols and C_{60} with radical species generated from methyl linoleate under autoxidation condition, we propose two antioxidant mechanisms which are dependent on the number of hydroxyl groups.

2. Materials and Methods

2.1. Materials and Apparatuses. Fullerlenols $C_{60}(OH)_n$ ($n = 44$, 12, 24, 26, 36, and 44) were synthesized by the previously reported procedures using hydrogen peroxide [12, 13] and $C_{60}(OH)_{26}$ was synthesized by the modified method with a shorter reaction time (methods A and A'). Fullerenol $C_{60}(OH)_{\sim 24}$ prepared from $C_{60}Br_{24}$ was purchased from MTR Ltd. (method B). Fullerlenols $C_{60}(OH)_n$ ($n = 12$ and 8) were synthesized by the modification of the literature method using oleum (method C) [19]. Fullerene C_{60} was purchased from Frontier Carbon Corporation as nanom purple ST (99%).

β -Carotene, linoleic acid (>99%), catechin mixture, isoflavone mixture, coenzyme Q10 (as ubiquinone-10),

curcumin, and α -lipoic acid were purchased from Wako Pure Chemical Industries, Ltd. Other reagents and organic solvents as well as pure water were all commercially available and used as received. UV-visible spectra were measured on a JASCO V-550 equipped with a thermal controller. LCMS analysis was performed on a SHIMADZU LCMS-2010EV. Matrix assisted laser desorption ionization time-of-flight mass spectra (MALDI-TOF-MS) were measured on a Bruker autoflex III.

2.2. β -Carotene Bleaching Assay. The β -carotene bleaching assay was performed according to an optimally modified procedure [2, 3]. Chloroform solutions of 11 μ L of β -carotene (1.0 mg/mL, 8.2 μ M), 4.4 μ L of linoleic acid (0.1 g/mL, 628 μ M), and 22 μ L of Tween 40 (0.2 g/mL) were mixed in a quartz cell equipped with a screw-on cap and then the solvent was removed in vacuo. The residual emulsion was immediately diluted with 2.4 mL of phosphate buffer solution (0.02 M, pH = 7.01), and 0.1 mL of antioxidant (0–20 μ M) in deionized water ($C_{60}(OH)_{\sim 24}$, 36, and 44) or DMSO ($C_{60}(OH)_8$, 12, and 26) was added to the diluted mixture. The solution was mixed well and heated at 50°C under air in a quartz cell on a UV spectrometer in order to monitor the decrease in the absorbance of β -carotene at 460 nm.

3. Results and Discussion

The discoloration rate in the presence of fullerene (R_f) is defined as (1), where k_{obs} is an observed pseudo-first-order rate constant, and k_c and k_f are rate constants for the reaction of β -carotene and fullerene with radical species (represented by LOO^*), respectively. Because the concentration of radical species must be considerably low and if it is approximated as a constant, the rate obeys a pseudo-first-order rate law with a constant of k_{obs} . When fullerene is absent as a control (i.e.,

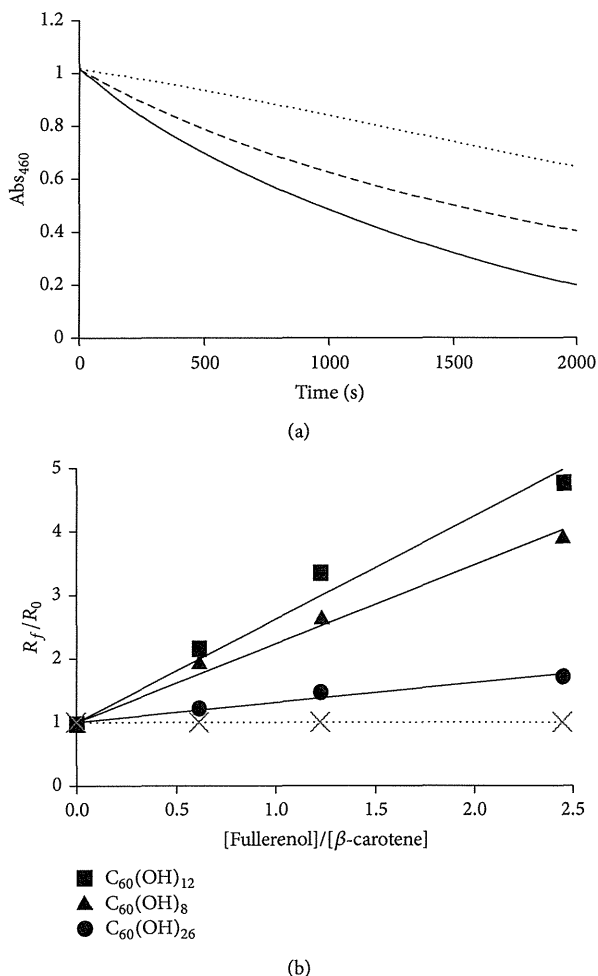


FIGURE 2: (a) Time course of the discoloration of β -carotene induced by autoxidation of linoleic acid under air at 50°C in the absence (solid line for control) or the presence of fullerenols (dotted line for $\text{C}_{60}(\text{OH})_{12}$ and dashed line for $\text{C}_{60}(\text{OH})_8$ in $10\ \mu\text{M}$) by monitoring of UV absorbance at 460 nm. (b) Plots of the ratio of β -carotene bleaching (discoloration) rates in the presence (R_f) or absence (R_0) of fullereneol R_f/R_0 versus the ratio of concentration [fullereneol]/[β -carotene] for various fullerenols: marked by square for $\text{C}_{60}(\text{OH})_{12}$, triangle for $\text{C}_{60}(\text{OH})_8$, and circle for $\text{C}_{60}(\text{OH})_{26}$. The slope of each linear regression line corresponds to the relative radical scavenging rate constant k_{rel} of fullerenols relative to β -carotene ($=k_f/k_c$). The dotted horizontal line indicates the value in the absence of antioxidant as a control ($R_f = R_0$ at any concentration; $k_{\text{rel}} = 0$).

[fullerene] = 0), the discoloration rate of β -carotene is defined as R_0 . Consider

$$\begin{aligned}
 R_f &= \frac{-d[\beta\text{-carotene}]}{dt} = k_{\text{obs}}[\beta\text{-carotene}] \\
 &= k_c[\beta\text{-carotene}] \\
 &\quad \times \left(\frac{k_c[\beta\text{-carotene}]}{k_c[\beta\text{-carotene}] + k_f[\text{fullerene}]} \right) [\text{LOO}^*].
 \end{aligned} \tag{1}$$

TABLE 1: The relative rate constant (k_{rel}) and antioxidant activity (%AOA) of fullerenols^a.

Compound	Method ^b	k_{rel}	%AOA at $10\ \mu\text{M}$
$\text{C}_{60}(\text{OH})_{44}$	A	1.54	66.0
$\text{C}_{60}(\text{OH})_{36}$	A'	0.80	52.7
$\text{C}_{60}(\text{OH})_{24}$	B	0.68	46.0
$\text{C}_{60}(\text{OH})_{26}$	A'	0.31	31.7
$\text{C}_{60}(\text{OH})_{12}$	C	1.62	70.1
$\text{C}_{60}(\text{OH})_8$	C	1.24	62.8
C_{60} ^c	[3]	0.79	50.0

^aThe reaction was conducted in anoxic conditions.

^bPreparation method described in Section 2.

^cPVP was used as a water solubilizer.

The β -carotene bleaching assay was carried out by previously reported method [2]. The decrease in absorbance of β -carotene is plotted as $\ln[(\text{Abs}_0)/(\text{Abs}_t)]$ versus reaction time that gave a linear regression line after a short presteady state (Figure 2(a)), consistent with the above approximation of the reaction as a pseudo-first-order kinetics (1).

By the plot of discoloration rate ratio R_f/R_0 to the various molar ratio of [fullerene]/[β -carotene] as shown in Figure 2(b), the ratio of rate constants k_f/k_c , which means the relative reactivity of fullerene to β -carotene (defined as k_{rel}), can be obtained as the slope of a linear line with the intercept of 1 as expressed by

$$\begin{aligned}
 \frac{R_f}{R_0} &= \frac{k_{\text{obs of fullerene}}}{k_{\text{obs of control}}} = \frac{k_c[\beta\text{-carotene}] + k_f[\text{fullerene}]}{k_c[\beta\text{-carotene}]} \\
 &= 1 + \frac{k_f}{k_c} \frac{[\text{fullerene}]}{[\beta\text{-carotene}]}, \quad \left(\frac{k_f}{k_c} = k_{\text{rel}} \right).
 \end{aligned} \tag{2}$$

The R_f/R_0 plots for $\text{C}_{60}(\text{OH})_8$, $\text{C}_{60}(\text{OH})_{12}$, and $\text{C}_{60}(\text{OH})_{26}$ exhibited that the highest k_{rel} value of 1.62 (i.e., 1.62 times reactive toward the present radical species relative to β -carotene) was observed for $\text{C}_{60}(\text{OH})_{12}$. The k_{rel} values as well as %AOA at $10\ \mu\text{M}$ of various fullerenols were summarized in Table 1. The antioxidant activity expressed using %AOA was defined by (3). The fullerenols having higher k_{rel} values showed higher values of %AOA. The %AOA is convenient to express the antioxidant activity using the value in the range from 0 (low) to 100 (high). However, it should be noted that the value of %AOA is concentration-dependent and the value of k_{rel} is not. Consider

$$\% \text{AOA} = \frac{(k_{\text{obs of control}}) - (k_{\text{obs of sample}})}{k_{\text{obs of control}}} \times 100. \tag{3}$$

Fullerenols $\text{C}_{60}(\text{OH})_n$ having ca. 10 ($n = 8$ and 12) or ca. 40 (36 and 44) hydroxyl groups showed somewhat high antioxidant activity as compared with those having ca. 25 (24 and 26). Lowly hydroxylated fullerene (ca. 10) showed high antioxidant activity probably because of the remaining relatively high π -conjugation in C=C double bonds, such as high HOMO and low LUMO, which is favourable for the

TABLE 2: The relative rate constant (k_{rel}) and antioxidant activity (%AOA) of naturally occurring antioxidants^{a,b}.

Compound	k_{rel}	%AOA at 10 μ M
Catechin	4.95	80.2
$C_{60}(OH)_{44}$	1.54	66.0
β -Carotene	1.00	—
Isoflavone	0.68	35.6
Coenzyme Q10	0.50	29.1
Curcumin	0.26	17.7
α -Lipoic acid	0.10	7.4

^aThe reaction was conducted in anoxic conditions.

^bData from [18].

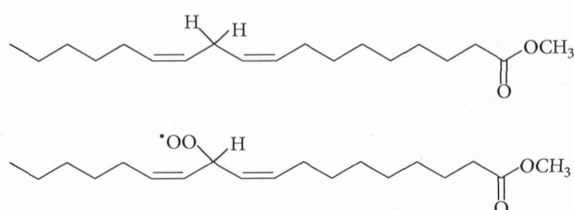
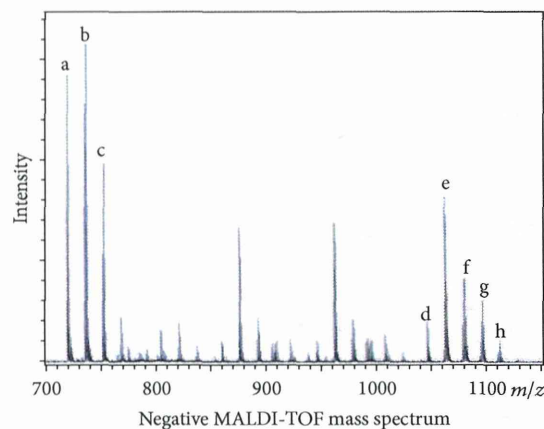


FIGURE 3: Structure of methyl linoleate (ML) and its peroxy radical (MLOO*).

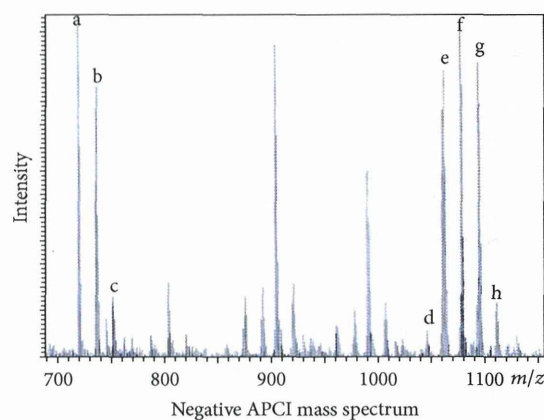
efficient molecular orbital interaction with the radical SOMO. Therefore, the activity decreased with the increasing number of hydroxyl groups, thus decreasing π -conjugation, up to ca. 25. However, surprisingly, the activity again increased with the increasing number of hydroxyl groups up to ca. 40 as highly hydroxylated ones. The present result suggests that the antioxidant mechanism of highly hydroxylated fullerenes may be different from those of lowly hydroxylated ones (vide infra).

For the comparison, the antioxidant activities of representative naturally occurring antioxidants measured by the same procedure were summarized in Table 2 [18]. Catechin showed the extremely high k_{rel} and %AOA values among those tested. Fullerenol $C_{60}(OH)_{44}$ also exhibited relatively high radical scavenging activity, slightly higher even than β -carotene, while curcumin and α -lipoic acid showed poor values in the present β -carotene bleaching assay.

General antioxidants are mainly categorized into three types according to their antioxidant mechanism, such as (i) electron donating type (reductant like ascorbic acid), (ii) hydrogen donating type (antioxidant having reactive hydrogen atom like phenolic -OH group of catechin), and (iii) radical trapping type (antioxidant having highly conjugated C=C double bonds like β -carotene) [20]. To investigate the antioxidant mechanism of fullerene, the reaction of C_{60} with methyl linoleate (ML) under autoxidation condition [21], heating with 300 equivalent excess of ML in toluene at 70°C for 3 days, was conducted as a model reaction. Because of the technical problems on solubility and mass detectability, the employment of linoleic acid failed. Both by MALDI-TOF-MS and by LC-MS with APCI negative mode analyses of the crude reaction mixture, the peroxy



(a)



(b)

Peak	m/z (MALDI/APCI)	Ion
a	720/720	C_{60}^-
b	737/737	$C_{60}(OH)^-$
c	753/753	$C_{60}O(OH)^-$
d	1045/1046	$C_{60}(OOML)^-$
e	1061/1062	$C_{60}O(OOML)^-$
f	1078/1078	$C_{60}O_2(OOML)^-$
g	1095/1095	$C_{60}O_3(OOML)^-$
h	1111/1111	$C_{60}O_4(OOML)^-$

(b)

FIGURE 4: Mass spectra of the crude product on the reaction of C_{60} with an excess amount of methyl linoleate by heating under air.

radical of methyl linoleate (MLOO*) was revealed to give fullerene multioxides ($C_{60}O_n$) and their radical addition products [$C_{60}(O)_n(OOML)_m$] along with their fragment peaks (Figures 3 and 4). This could be a part of evidence for a radical trap mechanism of fullerene C_{60} . On the other hand, no peaks derived from MLOO* were obtained in the reaction of $C_{60}(OH)_8$ with ML by mass and NMR spectroscopy. Although it failed to detect the product in this case, the disappearance of mass peaks corresponding to the starting $C_{60}(OH)_8$, which were observed before the reaction, implied that the fullerenol reacted with ML.

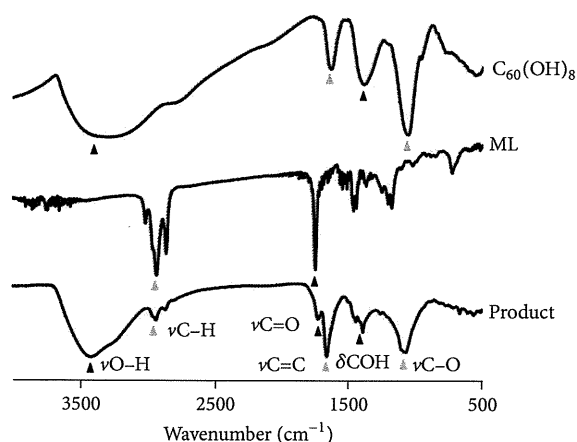


FIGURE 5: IR spectra of the crude product on the reaction of fullerene $C_{60}(OH)_8$ with methyl linoleate (ML) under autoxidation condition along with those of the starting materials.

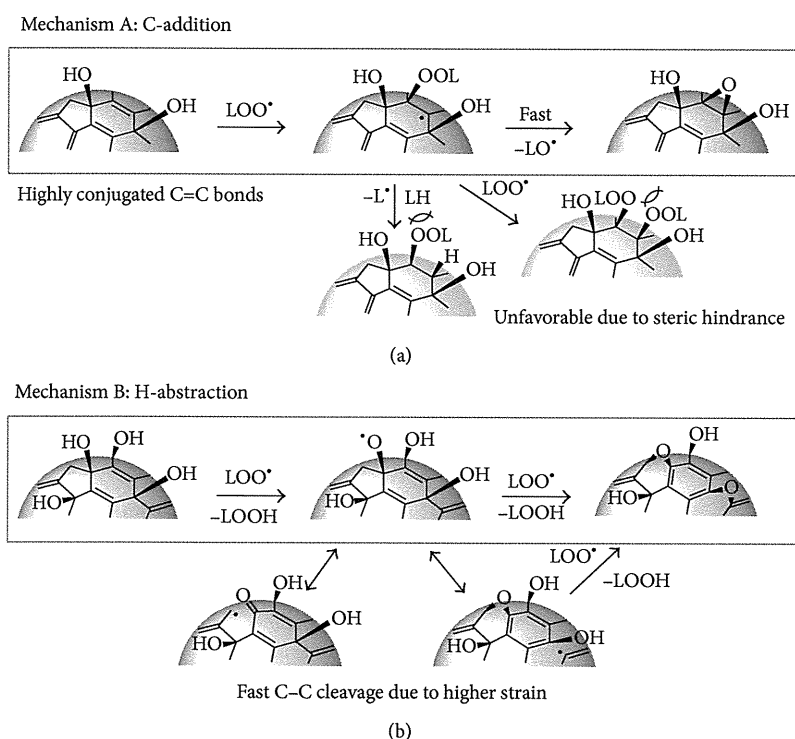


FIGURE 6: Possible mechanisms for lipid peroxyl radical (LOO^{\bullet}) scavenging by fullerenes $C_{60}(OH)_n$: (a) addition to C=C double bonds for less hydroxylated fullerenes and (b) H-abstraction from -OH group for highly hydroxylated ones.

Instead of the failed mass analysis, the reaction product of fullerene $C_{60}(OH)_8$ with ML was analysed by IR spectroscopy (Figure 5). Even after reprecipitation of the product from diethyl ether/hexane = 9/1 followed by Florisil column chromatography with an eluent of THF, the small peak at ca. 1700 cm^{-1} assigned for $\nu C=O$ was observed along with the peaks at ca. 2900 cm^{-1} assigned for $\nu C-H$. These signals may appear by the addition of $MLOO^{\bullet}$ which has an ester moiety

or by the hydrogen abstraction from hydroxyl group with the subsequent carbonyl group formation (vide infra).

By considering the above results, we proposed two possible radical scavenging mechanisms of fullerenes as shown in Figure 6. One is "C-addition" type, which includes the peroxyl radical addition to a conjugated C=C double bond (mechanism A), and the other is "H-abstraction" type, which includes hydrogen atom abstraction from -OH group and the

subsequent skeletal rearrangement of fullereryl cage forming ether bridge (mechanism B). Lowly hydroxylated fullerlenols $C_{60}(OH)_n$ ($n = \text{ca. } 10$) which have enough π -conjugated double bonds probably favour the “C-addition” mechanism similar to the pristine C_{60} . By contrast, highly hydroxylated fullerlenols $C_{60}(OH)_n$ ($n = \text{ca. } 40$) seem to be relatively difficult to undergo the C-addition of $MLOO^\bullet$ because they have less and unreactive double bonds in addition to the larger steric hindrance from the crowded hydroxyl groups. The latter mechanism is the same as catechin (polyphenol) type and it is supported by the fact that some fullerlenols have acidic (similar to phenolic) hydroxyl groups. Because highly hydroxylated fullerlenols have larger strain on fullereryl cage due to the conversion of many sp^2 carbons into sp^3 carbons by hydroxylation, H-abstraction may be followed by the subsequent skeletal rearrangement on C_{60} cage to release the strain energy, forming some ether bridge. Fullerlenols $C_{60}(OH)_n$ ($n = \text{ca. } 24$) result in poor antioxidant activity probably due to the lack of both effects.

Finally, we also measured the antioxidant activity of several alcohols and phenols. Under the same condition of β -carotene bleaching assay, ethanol, *t*-butyl alcohol, benzyl alcohol, allyl alcohol, phenol, and *p*-bromophenol did not show antioxidant activity in spite of the existence of hydroxyl groups and unsaturated structures. The result clearly suggests the importance of high conjugation and distorted structure of fullerlenols for the antioxidant activity in β -carotene bleaching assay.

4. Conclusions

In conclusion, we systematically evaluated the antioxidant activity of variously hydroxylated fullerlenols by β -carotene bleaching assay. The antioxidant activity %AOA was varied from 32% to 70% by changing the number of hydroxyl groups and both lowly hydroxylated $C_{60}(OH)_{12}$ (70.1%) and highly hydroxylated $C_{60}(OH)_{44}$ (66.0%) showed relatively high antioxidant activity. The obtained relative radical scavenging rate of fullerene k_{rel} toward radical species derived from linoleic acid under autoxidation condition indicated that these fullerlenols reacted 1.62 and 1.54 times faster than β -carotene, respectively. By the product analysis using the model reaction of C_{60} and methyl linoleate under autoxidation condition, we detected several mass peaks of radical scavenged fullerene derivatives as well as the IR spectra. These results suggest that the high π -conjugation and the strained structure of fullerlenol are responsible for the high radical scavenging reactivity and thus we proposed two possible antioxidant mechanisms, such as C-addition type and H-abstraction type, which are dependent on the number of hydroxyl groups.

Conflict of Interests

The authors declare that there is no conflict of interests regarding the publication of this paper.

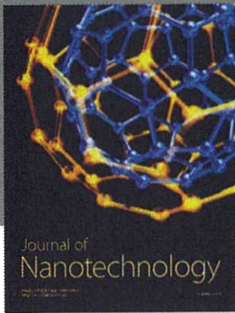
Acknowledgments

This work was supported by Health Labor Sciences Research Grants from MHLW, Japan. The authors thank Dr. H. Aoshima (Vitamin C60 BioResearch Corporation) for helpful discussion.

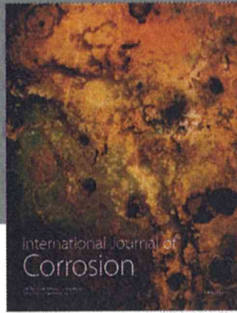
References

- [1] P. J. Krusic, E. Wasserman, P. N. Keizer, J. R. Morton, and K. F. Preston, “Radical reactions of C_{60} ,” *Science*, vol. 254, no. 5035, pp. 1183–1185, 1991.
- [2] H. Takada, K. Kokubo, K. Matsubayashi, and T. Oshima, “Antioxidant activity of supramolecular water-soluble fullerlenes evaluated by β -carotene bleaching assay,” *Bioscience, Biotechnology and Biochemistry*, vol. 70, no. 12, pp. 3088–3093, 2006.
- [3] K. Matsubayashi, T. Goto, K. Togaya, K. Kokubo, and T. Oshima, “Effects of pin-up oxygen on [60]fullerene for enhanced antioxidant activity,” *Nanoscale Research Letters*, vol. 3, no. 7, pp. 237–241, 2008.
- [4] L. Y. Chiang, F.-J. Lu, and J.-T. Lin, “Free radical scavenging activity of water-soluble fullerlenols,” *Journal of the Chemical Society, Chemical Communications*, no. 12, pp. 1283–1284, 1995.
- [5] S. Kato, H. Aoshima, Y. Saitoh, and N. Miwa, “Highly hydroxylated or γ -cyclodextrin-bicapped water-soluble derivative of fullerene: the antioxidant ability assessed by electron spin resonance method and β -carotene bleaching assay,” *Bioorganic and Medicinal Chemistry Letters*, vol. 19, no. 18, pp. 5293–5296, 2009.
- [6] Y. Saitoh, L. Xiao, H. Mizuno et al., “Novel polyhydroxylated fullerene suppresses intracellular oxidative stress together with repression of intracellular lipid accumulation during the differentiation of OP9 preadipocytes into adipocytes,” *Free Radical Research*, vol. 44, no. 9, pp. 1072–1081, 2010.
- [7] Y. Saitoh, A. Miyanishi, H. Mizuno et al., “Super-highly hydroxylated fullerene derivative protects human keratinocytes from UV-induced cell injuries together with the decreases in intracellular ROS generation and DNA damages,” *Journal of Photochemistry and Photobiology B*, vol. 102, no. 1, pp. 69–76, 2011.
- [8] Y. Saitoh, H. Mizuno, L. Xiao, S. Hyoudou, K. Kokubo, and N. Miwa, “Polyhydroxylated fullerene $C_{60}(OH)_{44}$ suppresses intracellular lipid accumulation together with repression of intracellular superoxide anion radicals and subsequent PPAR γ 2 expression during spontaneous differentiation of OP9 preadipocytes into adipocytes,” *Molecular and Cellular Biochemistry*, vol. 366, no. 1–2, pp. 191–200, 2012.
- [9] G. D. Nielsen, M. Roursgaard, K. A. Jensen, S. S. Poulsen, and S. T. Larsen, “In vivo biology and toxicology of fullerlenes and their derivatives,” *Basic & Clinical Pharmacology & Toxicology*, vol. 103, no. 3, pp. 197–208, 2008.
- [10] J. Gao, Y. Wang, K. M. Folta et al., “Polyhydroxy fullerlenes (fullerols or fullerlenols): beneficial effects on growth and lifespan in diverse biological models,” *PLoS ONE*, vol. 6, no. 5, Article ID e19976, 8 pages, 2011.
- [11] Z. Chen, L. Ma, Y. Liu, and C. Chen, “Applications of functionalized fullerlenes in tumor theranostics,” *Theranostics*, vol. 2, no. 3, pp. 238–250, 2012.
- [12] K. Kokubo, S. Shirakawa, N. Kobayashi, H. Aoshima, and T. Oshima, “Facile and scalable synthesis of a highly hydroxylated water-soluble fullerlenol as a single nanoparticle,” *Nano Research*, vol. 4, no. 2, pp. 204–215, 2011.

- [13] K. Kokubo, K. Matsubayashi, H. Tategaki, H. Takada, and T. Oshima, "Facile synthesis of highly water-soluble fullerenes more than half-covered by hydroxyl groups," *ACS Nano*, vol. 2, no. 2, pp. 327–333, 2008.
- [14] H. Ueno, K. Kokubo, E. Kwon, Y. Nakamura, N. Ikuma, and T. Oshima, "Synthesis of a new class of fullerene derivative $\text{Li}^+@C_{60}O^-(\text{OH})_7$ as a "Cation-encapsulated anion nanoparticle," *Nanoscale*, vol. 5, pp. 2317–2321, 2013.
- [15] G. Zhang, Y. Liu, D. Liang, L. Gan, and Y. Li, "Facile synthesis of isomerically pure fullerlenols and formation of spherical aggregates from $C_{60}(\text{OH})_8$," *Angewandte Chemie International Edition*, vol. 49, pp. 5293–5295, 2010.
- [16] M. S. Al-Saikhan, L. R. Howard, and J. C. Miller Jr., "Antioxidant activity and total phenolics in different genotypes of potato (*Solanum tuberosum*, L.)," *Journal of Food Science*, vol. 60, pp. 341–347, 1995.
- [17] A. Djordjevic, J. M. Canadanovic-Brunet, M. Vojinovic-Miloradov, and G. Bogdanovic, "Antioxidant properties and hypothetical radical mechanism of fullereneol $C_{60}(\text{OH})_{24}$," *Oxidation Communications*, vol. 27, no. 4, pp. 806–812, 2004.
- [18] H. Aoshima, K. Togaya, T. Goto et al., "Evaluation of antioxidant activity of fullerenes and their inhibition effects on photodegradation of cosmetic ingredients," *Journal of Japanese Cosmetic Science Society*, vol. 33, pp. 149–154, 2009.
- [19] L. Y. Chiang, L.-Y. Wang, J. W. Swirczewski, S. Soled, and S. Cameron, "Efficient synthesis of polyhydroxylated fullerene derivatives via hydrolysis of polycyclosulfated precursors," *Journal of Organic Chemistry*, vol. 59, no. 14, pp. 3960–3968, 1994.
- [20] G. W. Burton and K. U. Ingold, " β -Carotene: an unusual type of lipid antioxidant," *Science*, vol. 224, no. 4649, pp. 569–573, 1984.
- [21] K. Fukuzumi, N. Ikeda, and M. Egawa, "Phenothiazine derivatives as new antioxidants for the autoxidation of methyl linoleate and their reaction mechanisms," *Journal of the American Oil Chemists' Society*, vol. 53, no. 10, pp. 623–627, 1976.



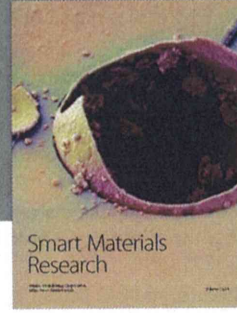
Journal of
Nanotechnology



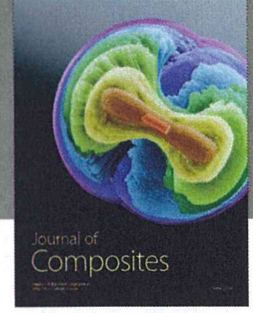
International Journal of
Corrosion



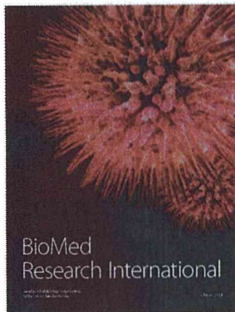
International Journal of
Polymer Science




Smart Materials
Research



Journal of
Composites

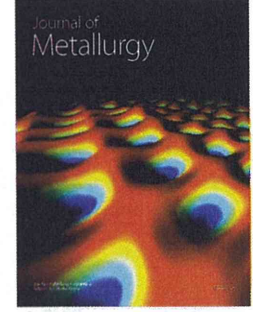


BioMed
Research International

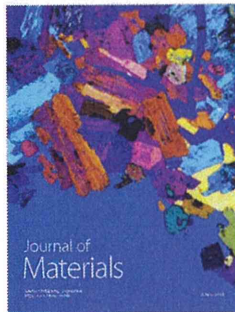


Hindawi

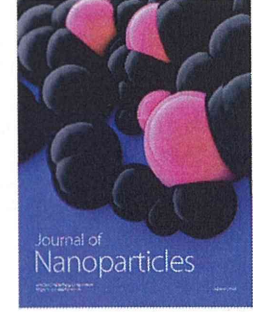
Submit your manuscripts at
<http://www.hindawi.com>



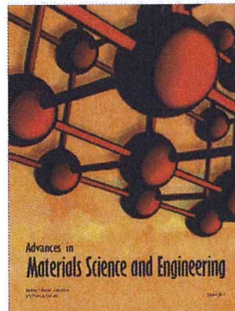
Journal of
Metallurgy



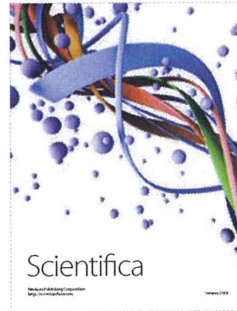
Journal of
Materials



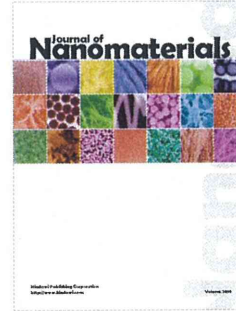
Journal of
Nanoparticles



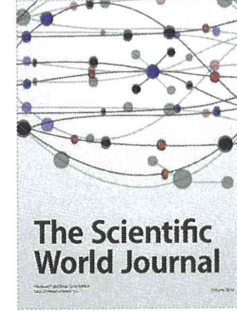
Advances in
Materials Science and Engineering



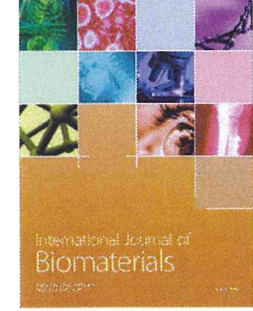
Scientifica



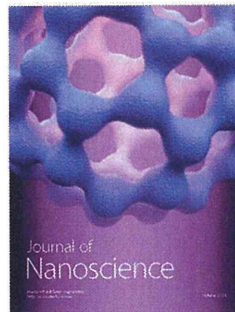
Journal of
Nanomaterials



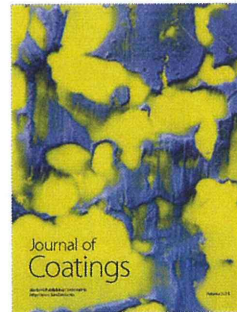
The Scientific
World Journal



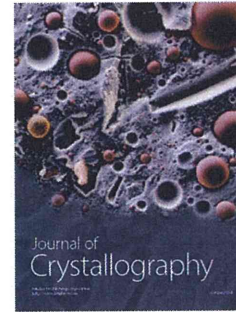
International Journal of
Biomaterials



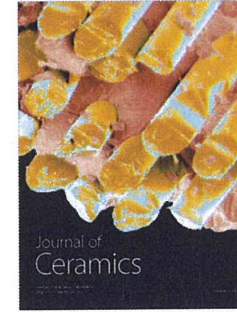
Journal of
Nanoscience



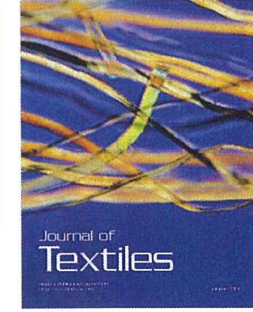
Journal of
Coatings



Journal of
Crystallography



Journal of
Ceramics



Journal of
Textiles



Effect of chemical modification on the ability of pyrrolidinium fullerene to induce apoptosis of cells transformed by JAK2 V617F mutant



Megumi Funakoshi-Tago ^{a,*}, Masaki Tsukada ^a, Toshiro Watanabe ^a, Yuka Mameda ^a, Kenji Tago ^b, Tomoyuki Ohe ^c, Shigeo Nakamura ^d, Tadahiko Mashino ^c, Tadashi Kasahara ^a

^a Department of Biochemistry, Faculty of Pharmacy, Keio University, 1-5-30 Shibakoen, Minato-ku, Tokyo 105-8512, Japan

^b Division of Structural Biochemistry, Department of Biochemistry, Jichi Medical University, 3311-1 Yakushiji, Shimotsuke-shi, Tochigi-ken 329-0498, Japan

^c Department of Medicinal Chemistry and Bio-organic Chemistry, Faculty of Pharmacy, Keio University, 1-5-30 Shibakoen, Minato-ku, Tokyo 105-8512, Japan

^d Department of Chemistry, Nippon Medical School, 2-297-2 Kosugi-cho, Nakahara-ku, Kawasaki, Kanagawa 211-0063, Japan

ARTICLE INFO

Article history:

Received 7 October 2013

Received in revised form 26 February 2014

Accepted 26 February 2014

Available online 12 March 2014

Keywords:

JAK2

V617F mutation

Myeloproliferative neoplasms

Pyrrolidinium fullerene

ASK1

JNK

ABSTRACT

JAK2 V617F mutant, a gene responsible for human myeloproliferative neoplasms (MPNs), causes not only cellular transformation but also resistance to various anti-cancer drugs. We previously reported that pyrrolidinium fullerene markedly induced the apoptosis of JAK2 V617F mutant-induced transformed cells through the reduction of apoptosis signal-regulating kinase 1 (ASK1), following inhibition of the c-Jun N-terminal kinase (JNK) pathway. In the current study, we found that the replacement of the 2-hydrogen atom (–H) or N-methyl group (–CH₃) by the butyl group (–C₄H₉) caused the more than 3-fold potent cytotoxic effects on cells transformed by the JAK2 V617F mutant. Strikingly, these chemical modification of pyrrolidinium fullerene resulted in more marked reduction of ASK1 protein and a more potent inhibitory effect on the JNK signaling cascade. On the other hand, when modified with a longer alkyl group, the derivatives lacked their cytotoxicity. These observations clearly indicate that the modification of pyrrolidinium fullerene with a suitable length of alkyl group such as butyl group enhances its apoptotic effect through inhibition of the ASK1-MKK4/7-JNK pathway.

© 2014 Elsevier B.V. All rights reserved.

1. Introduction

The myeloproliferative neoplasms (MPNs), which include polycythemia vera (PV), essential thrombocytosis (ET) and primary myelofibrosis (PMF), are clonal hematopoietic stem cell diseases characterized by uncontrolled proliferation of terminally differentiated myeloid cells. A somatic mutation of the tyrosine kinase Janus kinase 2 (JAK2) gene was identified in more than 90% of PV patients and in approximately 50% of ET and PMF patients. In the majority of MPN patients, the JAK2 gene has a homozygous G → T transversion, which results in a valine-to-phenylalanine substitution at codon 617 of JAK2 (V617F) [1–3].

Previously, we found that the JAK2 V617F mutant induces the cytokine-independent survival of erythroid progenitor cells [4]. The JAK2 V617F mutant was reported to induce the activation of signaling pathways, signal transduction and activator of transcription 3 (STAT3)

and STAT5 and kinases, Akt, extracellular signal-regulated kinase (ERK) and c-Jun N-terminal kinase (JNK) in a cytokine-independent manner. We demonstrated that STAT5, Akt and JNK are critical signal transducers for the proliferation and the transforming ability induced by JAK2 V617F mutant [5–7]. In addition, it was shown that cells transformed by the JAK2 V617F mutant exhibited resistance to various anti-cancer drugs, such as bleomycin (BLM), which generates DNA double-strand breaks, and mitomycin C (MMC) and cisplatin (CDDP), which are DNA cross-linking drugs [8–11], suggesting that the JAK2 V617F mutant causes not only the activation of survival signals against apoptosis induced by cytokine removal but also the resistance to various anti-cancer drugs. Therefore, the rapid development of effective therapeutic drugs for MPNs is required.

Fullerene (C₆₀) was discovered by Kroto et al. in 1985 as the third allotropic form of carbon after diamond and graphite [12]. Fullerene is a spherical molecule 0.7 μm in diameter and a new type of organic compound with a cage-like structure [13]. Chemical modification with several hydrophilic groups increases the solubility of fullerene, and the derivatives of water-soluble fullerene were reported to possess various biological and pharmacological properties [14–18]. As a typical derivative, pyrrolidinium fullerene exhibits anti-proliferative activity to various cancer cells [19]. Previously, we reported that pyrrolidinium fullerene markedly induced apoptotic cell death of cells transformed by the JAK2 V617F mutant through reduction of the protein expression of apoptosis

Abbreviations: ASK1, apoptosis signal-regulating kinase 1; c-IAP1, cellular inhibitor of apoptosis protein 1; DCFH, dichlorodihydrofluorescein; DMSO, dimethyl sulfoxide; Epo, erythropoietin; ERK, extracellular signal-regulated kinase; EpoR, erythropoietin receptor; ET, essential thrombocytosis; JAK2, Janus kinase 2; JNK, c-Jun N-terminal kinase; MKK4/7, mitogen-activated protein kinase kinase 4/7; MPNs, myeloproliferative neoplasms; PMF, primary myelofibrosis; PV, polycythemia vera; STAT, signal transducers and activators of transcription; ROS, reactive oxygen species.

* Corresponding author. Tel./fax: +81 3 5400 2697.

E-mail address: tago-mg@pha.keio.ac.jp (M. Funakoshi-Tago).

signal-regulating kinase 1 (ASK1) and inhibition of the JNK pathway [20]. ASK1, one of the mitogen-activated protein kinase kinases (MAPKKKs), was previously demonstrated to stimulate the JNK signaling cascade mediating the activation of JNK upstream kinases, named MKK4/7 [21].

In the current study, we focused on the relationship between the chemical structure of the derivatives of pyrrolidinium fullerene and their apoptotic effects. Our study suggests the possibility that the chemical modification of fullerene would emphasize their utility as anti-cancer drugs.

2. Materials and methods

2.1. Chemicals and reagents

Pyrrolidinium fullerene and its derivatives were synthesized as previously described [15,17,19]. Anti β -actin antibody and anti-HA antibody (3F10) were purchased from Santa Cruz Biotechnology (Santa Cruz, CA) and Roche (Indianapolis, IN), respectively. Anti-phospho JAK2 antibody (Y1007/Y1008), anti-phospho-STAT3 antibody (Y705), anti-STAT3 antibody, anti-phospho-STAT5 antibody (Y694), anti-STAT5 antibody, anti-phospho-ERK1/2 antibody (T202/Y204), anti-ERK1/2

antibody, anti-phospho-Akt (S473), anti-Akt antibody, anti-ASK1 antibody, anti-phospho-MKK4 antibody (S257/T261), anti-MKK4 antibody, anti-phospho-MKK7 antibody (S271/T275), anti-MKK7 antibody, anti-phospho-JNK antibody (T183/Y185), anti-JNK antibody and anti-cleaved caspase 3 antibody were purchased from Cell Signaling Technology (Danvers, MA, USA). Peroxidase-conjugated secondary antibodies were from Dako (Glostrup, Denmark). 2', 7'-dichlorofluorescein diacetate (DCFH-DA) and α -tocopherol were purchased from Sigma Inc. (St. Louis, MO).

2.2. Retroviral infection and cell cultures

Ba/F3 cells were infected with retroviruses coding a mutant of murine JAK2 c-HA (V617F) with murine EpoR as described previously [4]. The cells were cultured in RPMI 1640 medium supplemented with 10% fetal bovine serum (BioWest, Nuaillé, France), 100 units/ml penicillin (Nacalai Tesque, Tokyo, Japan) and 100 μ g/ml streptomycin (Nacalai Tesque).

2.3. Western blotting

Cells were harvested in ice-cold PBS and lysed in Nonidet P-40 lysis buffer (50 mM Tris-HCl, pH 8.0, 120 mM NaCl, 1 mM EDTA pH 8.0, 0.5%

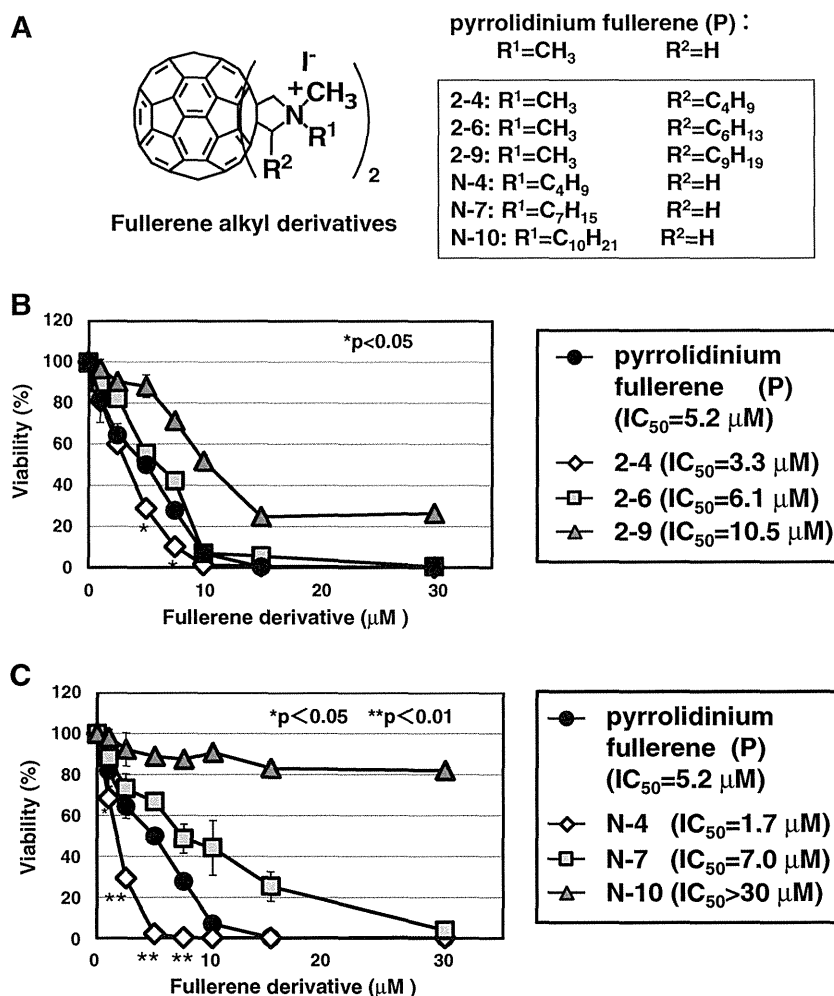


Fig. 1. Pyrrolidinium fullerene and its derivatives exhibit cytotoxicity to VF-Ba/F3 cells. (A) Structures of fullerene derivatives. Pyrrolidinium fullerene (P) is C_{60} -bis *N,N*-dimethylpyrrolidinium iodide. In pyrrolidinium fullerene (P), the 2-hydrogen atom ($-\text{H}$) or *N*-methyl group ($-\text{CH}_3$) was substituted with various alkyl groups and named 2-4, 2-6, 2-9, N-4, N-7, and N-10, respectively. (B, C) VF-Ba/F3 cells were treated with different concentrations (1, 2.5, 5, 7.5, 10, 15, 30 μM) of pyrrolidinium fullerene (P) and its derivatives for 24 h. Cell viability was determined by trypan blue staining. Results are the mean \pm S.D. of three independent experiments. * and ** indicate significant differences at $p < 0.05$ and $p < 0.01$, respectively (vs pyrrolidinium fullerene (P)).

Nonidet P-40, 10 mM β -glycerophosphate, 2.5 mM NaF, 0.1 mM Na_2VO_4) supplemented with protease inhibitors. Denatured samples were resolved by SDS-PAGE and transferred to polyvinylidene difluoride membranes (Millipore, Billerica, MA). Membranes were probed using the designated antibodies and visualized with the ECL detection system (GE Healthcare, Little Chalfont, United Kingdom) [4].

2.4. Measurement of cell viability and cell cycle analysis

Transduced Ba/F3 cells were incubated with RPMI 1640 medium supplemented with 1% fetal bovine serum. Cells were treated with DMSO (0.1%) or various concentrations of pyrrolidinium fullerene derivatives for 24 h. Cell viability was checked by the trypan blue exclusion method. Cell cycle parameters were determined by flow-cytometry analysis using FACSCalibur (BD Biosciences, San Jose, CA) [5].

2.5. DNA fragmentation assay

Genomic DNA was prepared for gel electrophoresis as described previously [5]. Electrophoresis was performed on a 1% agarose gel in Tris/boric acid/EDTA buffer.

2.6. Measurement of ROS generation

Cells were incubated with DCFH-DA (2', 7'-dichlorodihydrofluorescein-DA), a permeable fluorescence probes (10 μM) for 15 min and washed with PBS. Then, cells were treated with each fullerene derivative at indicated concentration for 1 h, and the fluorescence intensity of oxidized DCF was monitored using FACSCalibur with the CELL Quest program as previously described [19]. To test the effect of α -tocopherol, cells were pre-treated with α -tocopherol (300 μM) for 1 h prior to the treatment with fullerene derivative.

2.7. Data presentation

All of the experiments were independently performed at least 3 times. Error bar means standard deviation (S.D.).

3. Results

3.1. Effects of pyrrolidinium fullerene derivatives on the viability of VF-Ba/F3 cells

A previous study showed that pyrrolidinium fullerene induced apoptotic cell death of Ba/F3 cells transformed by the JAK2 V617F mutant (VF-Ba/F3 cells) [20]. To test the effect of chemical modification on the cytotoxicity of pyrrolidinium fullerene, 6 types of derivatives were newly synthesized from pyrrolidinium fullerene as the lead compound. As shown in Fig. 1A, derivatives named 2-4, 2-6 and 2-9 are compounds in which the 2-hydrogen atom ($-\text{H}$) in pyrrolidinium fullerene was replaced by a butyl group ($-\text{C}_4\text{H}_9$), hexyl group ($-\text{C}_6\text{H}_{13}$) and nonyl group ($-\text{C}_9\text{H}_{19}$), respectively. In three other derivatives, named N-4, N-7 and N-10, the N-methyl group ($-\text{CH}_3$) in pyrrolidinium fullerene was replaced by a butyl group ($-\text{C}_4\text{H}_9$), heptyl group ($-\text{C}_7\text{H}_{15}$) and decyl group ($-\text{C}_{10}\text{H}_{21}$), respectively. First, we tested the effects of these two groups of derivatives on the viability of VF-Ba/F3 cells. Compared to original pyrrolidinium fullerene, 2-4 more effectively induced the cell death of VF-Ba/F3 cells, while the cytotoxicity of 2-6 and 2-9 was comparable and lower than the original compound, respectively. In the next derivative's group, only N-4 showed more effective cytotoxicity. The cytotoxicity of N-7 was lower than the original compound and N-10 had no effect on the viability of VF-Ba/F3 cells (Fig. 1C). JAK2 V617F mutant-transformed cells exhibited higher sensitivity against these two derivatives, 2-4 and N-4, than the original pyrrolidinium fullerene. IC_{50} of derivatives 2-4 and N-4 was 3.3 μM and 1.7 μM , respectively, while IC_{50} of pyrrolidinium fullerene was 5.2 μM .

3.2. Apoptosis induction of VF-Ba/F3 cells by pyrrolidinium fullerene derivatives

In the previous study, pyrrolidinium fullerene exhibited apoptotic effects on VF-Ba/F3 cells. Therefore, we tested whether the derivatives could induce apoptotic cell death of VF-Ba/F3 cells. As in the previous study, the original pyrrolidinium fullerene resulted in the accumulation of sub-G1 phase, an index to evaluate apoptosis in a dose-dependent

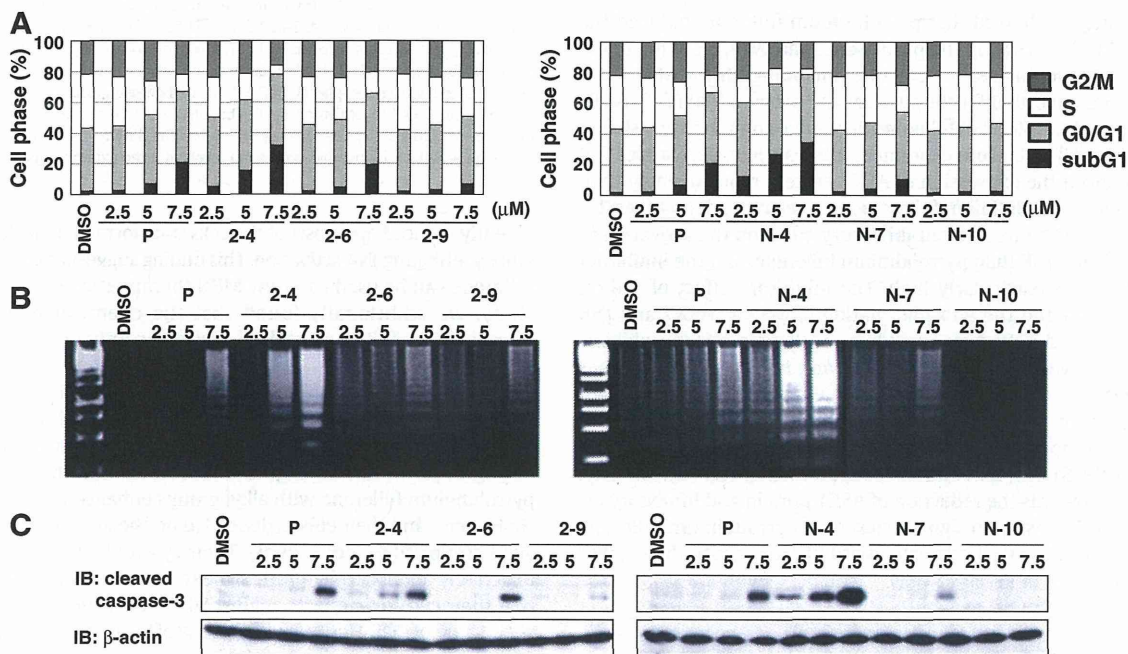


Fig. 2. Pyrrolidinium fullerene and its derivatives induce apoptosis of VF-Ba/F3 cells. VF-Ba/F3 cells were treated with DMSO (0.1%), pyrrolidinium fullerene (P) or its derivatives, 2-4, 2-6, 2-9, N-4, N-7, and N-10 (2.5, 5, 7.5 μM), for 24 h. (A) Cells were fixed, treated with propidium iodide and subjected to flow-cytometry analysis. (B) DNA was isolated from cells and subjected to agarose gel electrophoresis. (C) Cell lysates were prepared and immunoblotted with anti-cleaved caspase-3 antibody or anti- β -actin antibody.

manner (Fig. 2). In the first derivative's group, only 2-4 showed higher efficiency to induce Sub-G1 accumulation, while the others, 2-6 and 2-9, were comparable and weaker, respectively. Similarly, in the next derivative's group, only N-4 showed a higher apoptotic effect against VF-Ba/F3 cells. It is also notable that 2-4 and N-4 showed apoptotic effects at a lower concentration (5 μ M), and these observations well fitted the observed results in Fig. 1. The ladder pattern of DNA internucleosomal fragmentation and the cleavage of caspase-3 were other suitable indexes to evaluate apoptosis. We next tested the effects of derivatives of pyrrolidinium fullerene on DNA fragmentation and caspase-3 activation. DNA fragmentation was clearly detected in VF-Ba/F3 cells treated with 2-4 and N-4 at 5 μ M, while pyrrolidinium fullerene and 2-6 showed similar effects at a higher concentration (7.5 μ M) (Fig. 2B). Notably, derivatives 2-4 and N-4 showed similar effects on caspase-3 activation (Fig. 2C). These data clearly suggested that the chemical modification of pyrrolidinium fullerene with a butyl group at a suitable position enhances its cytotoxicity.

3.3. Pyrrolidinium fullerene derivatives caused apoptosis in ROS-independent manner

Next, we tested the ability of pyrrolidinium fullerene derivatives to induce ROS generation. Derivatives 2-4, 2-6 and N-4 comparably caused ROS generation like unmodified pyrrolidinium fullerene. On the other hand, derivative 2-9 exhibited slightly lower activity to induce ROS generation, and N-7 and N-10 failed to induce ROS generation in VF-Ba/F3 cells (Fig. 3A). Next, to test whether oxidative stress is involved in their cytotoxic effects against VF-Ba/F3 cells, the effect of an antioxidant, α -tocopherol was analyzed. Pretreatment with α -tocopherol significantly suppressed ROS generation induced by pyrrolidinium fullerene and its derivatives, 2-4, 2-6, 2-9 and N-4 (Fig. 3B). However, α -tocopherol failed to cancel their cytotoxic effects (Fig. 3C). These results suggest that fullerene derivatives cause apoptotic effects against VF-Ba/F3 cells through ROS-independent mechanisms.

3.4. Effects of pyrrolidinium fullerene derivatives on the expression of ASK1 protein and JNK signaling cascade in VF-Ba/F3 cells

Previously, we showed that pyrrolidinium fullerene reduced the expression level of ASK1 by the proteasome pathway, resulting in the inhibition of its downstream molecules, including MKK4, MKK7 and JNK, which are important for the survival and proliferation of VF-Ba/F3 cells [20]. Next, the effects of fullerene derivatives on the expression of ASK1 in VF-Ba/F3 cells were examined. Interestingly, derivatives 2-4 and N-4 reduced the expression of ASK1 protein more strongly than treatment with pyrrolidinium fullerene. Furthermore, derivatives 2-4 and N-4 exhibited a more potent inhibitory effect on the activation of MKK4, MKK7 and JNK than pyrrolidinium fullerene, and the inhibitory effect of N-4 was particularly high. The inhibitory effect of 2-6 on ASK1 expression and the phosphorylation of MKK4, MKK7 and JNK was equivalent to the effect of pyrrolidinium fullerene, and the inhibitory effect of 2-9 was lower than pyrrolidinium fullerene. On the other hand, derivatives N-7 and N-10 had little effect on ASK1 expression and activation of MKK4, MKK7 and JNK (Fig. 4A, B). On the other hand, these compounds failed to inhibit other signaling molecules including JAK2, STAT5, ERK and Akt (Supplemental Fig. 1S). Notably, the tendency towards the reduction of ASK1 protein and inhibitory effects on ASK1 downstream signals caused by pyrrolidinium fullerene and its derivatives are well correlated with the strength of their ability to induce apoptosis of VF-Ba/F3 cells.

4. Discussion

As reported previously, JAK2 V617F mutant-induced transformed cells show resistance to various anti-tumor drugs in comparison with untransformed cells [20]. Here, we showed that pyrrolidinium fullerene

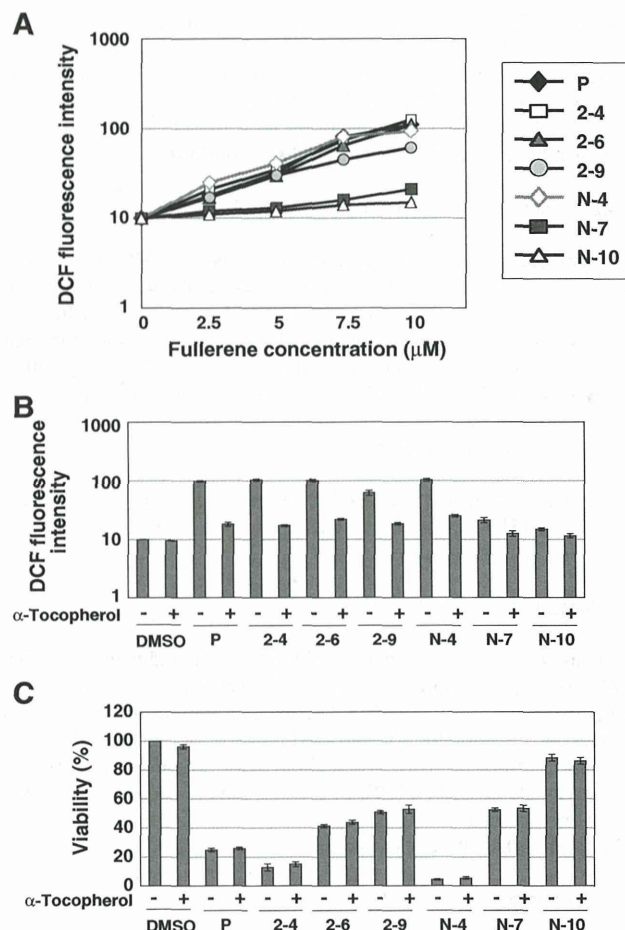


Fig. 3. Pyrrolidinium fullerene and derivatives 2-4 and N-4 induced apoptosis of VF-Ba/F3 cells independently of ROS production. (A) VF-Ba/F3 cells were incubated with DCFH-DA fluorescence probes (10 μ M) for 15 min and treated with DMSO (0.1%), pyrrolidinium fullerene or its derivatives, 2-4, 2-6, 2-9, N-4, N-7, and N-10 (2.5, 5, 7.5, 10 μ M), for 1 h. Oxidative stress was measured using DCFH-DA fluorescence probes. (B, C) VF-Ba/F3 cells were incubated with DCFH-DA fluorescence probes (10 μ M) for 15 min and then pre-incubated with α -tocopherol (300 μ M) for 1 h before exposure to DMSO (0.1%) or fullerene derivatives (7.5 μ M) for 1 h. (B) Oxidative stress was measured using DCFH-DA fluorescence probes. (C) Cell viability was determined by trypan blue staining. Data are the mean \pm S.D. of the relative expression levels in three experiments.

potently induced apoptosis of the cells transformed by JAK2 V617F mutant by inhibiting JNK activation. This finding suggests that pyrrolidinium fullerene can be used as a new MPN therapeutic drug. In the current study, we additionally found that the chemical modification of pyrrolidinium fullerene with a butyl group enhanced its cytotoxicity (Fig. 5).

It has been well established that fullerene derivatives show biological effects by mediating the production of ROS [19,20]. We also examined the effect of the modification of pyrrolidinium fullerene with alkyl groups of various lengths. It was found that the modification of pyrrolidinium fullerene with alkyl groups enhanced the cytotoxicity to HL-60 cells, and their effects depended on the length of the introduced alkyl groups (data not shown). Their cytotoxicity to HL-60 cells was effectively abolished by pretreatment with α -tocopherol, suggesting that their cytotoxic effects against HL-60 cells were mediated by the production of ROS. However, in the case of VF-Ba/F3 cells, pyrrolidinium fullerene modified with a butyl group caused the apoptotic effect, not through ROS production (Fig. 3). These findings clearly suggest that alkyl pyrrolidinium fullerenes cause cytotoxicity by affecting various signaling pathways, depending on the type of target cells. However,

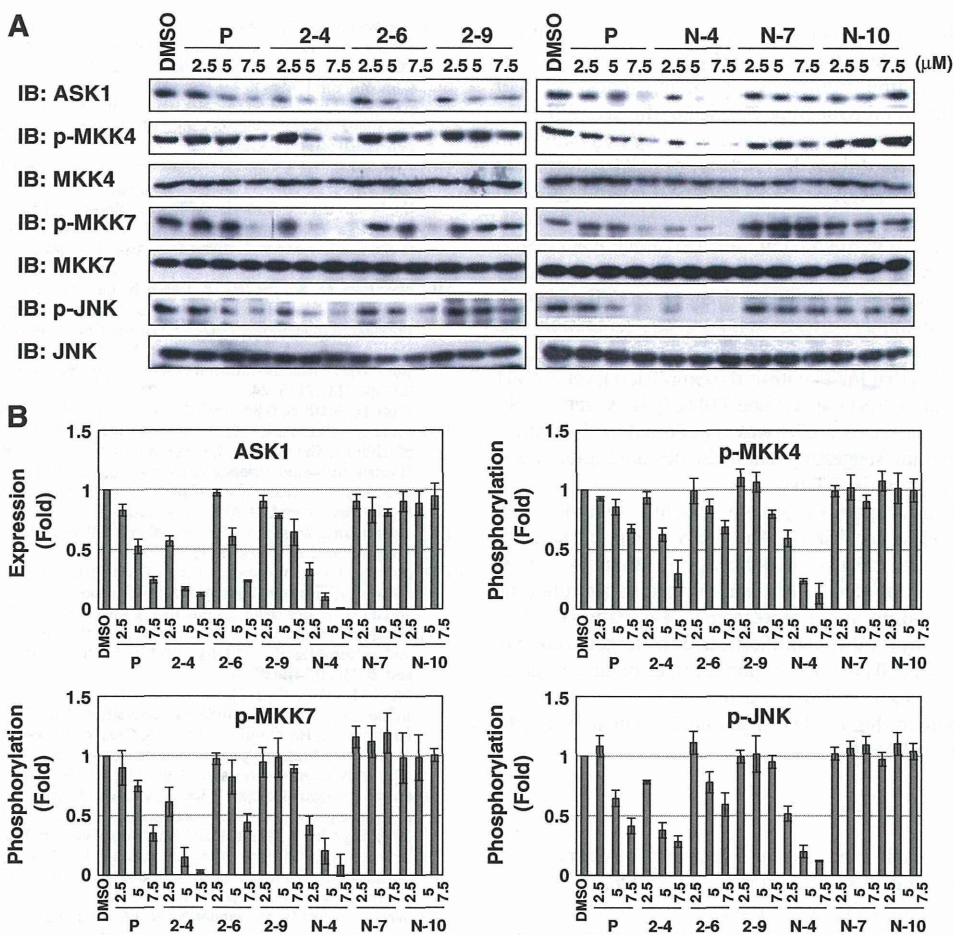


Fig. 4. Derivatives 2–4 and N–4 cause protein reduction of ASK1 and inhibit JNK signaling cascade. (A, B) VF-Ba/F3 cells were treated with DMSO (0.1%), pyrrolidinium fullerene (P), or its derivatives, 2–4, 2–6, 2–9, N–4, N–7, and N–10 (2.5, 5, 7.5 μM) for 16 h. (A) Cell lysates were immunoblotted with anti-ASK1 antibody, anti-phospho-MKK4 antibody (S257/T261), anti-MKK4 antibody, anti-phospho-MKK7 antibody (S271/T275), anti-MKK7 antibody, anti-phospho-JNK antibody (T183/Y185), anti-JNK antibody or anti-β-actin antibody. (B) The expression level of ASK1 was normalized with the expression level of β-actin. The phosphorylation levels of MKK4, MKK7 and JNK were normalized with the expression level of these molecules. The fold expression of ASK1 and the fold phosphorylation of MKK4, MKK7 and JNK are shown in graphs. Data are the mean ± S.D. of the relative expression levels in three experiments.

it is still unknown what causes the differences in the response to pyrrolidinium fullerene and its derivatives in target cells.

A number of studies have reported the importance of the JNK signaling cascade for anti-apoptotic and oncogenic signals. Previously,

we observed that a specific JNK inhibitor, SP600125, significantly induced the apoptosis of VF-Ba/F3 cells. In addition, inhibition of JNK reduced the expression of c-Myc, a proto-oncogene product contributing to the transforming activity of JAK2 V617F mutant [20–24]. The JNK

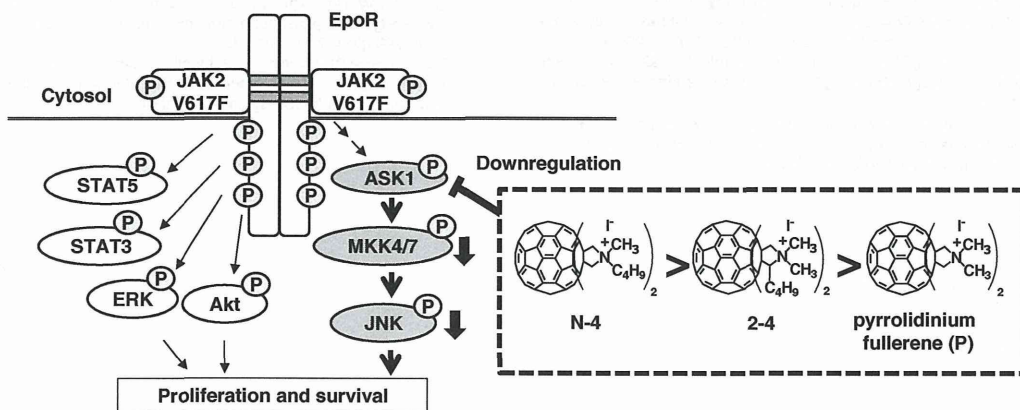


Fig. 5. Inhibitory mechanism of JAK2 V617F mutant-induced signaling pathway by pyrrolidinium fullerene derivatives. Pyrrolidinium fullerene (P) reduces the expression of ASK1, resulting in inhibition of the phosphorylation of MKK4, MKK7 and JNK, and induces apoptotic cell death of VF-Ba/F3 cells. The replacement of the 2-hydrogen atom (–H) or N-methyl group (–CH₃) with a butyl group (–C₄H₉) enhanced the ability of pyrrolidinium fullerene to induce apoptosis. In particular, replacement with a butyl group at 2-H more effectively enhanced the ability of pyrrolidinium fullerene to induce apoptosis.

signaling pathway has been reported to inactivate a pro-apoptotic protein, Bad, through its phosphorylation [25]. Although we did not test the effect of pyrrolidinium fullerene on the phosphorylation of Bad, this will be an important issue to be clarified in the near future.

Notably, we found that the cytotoxicity caused by pyrrolidinium fullerenes was well correlated with the tendency of ASK1 reduction in VF-Ba/F3 cells (Fig. 4). Previously, we showed that the down-regulation of ASK1 by pyrrolidinium fullerene was abolished by a proteasome inhibitor MG132, suggesting that pyrrolidinium fullerene caused ASK1 degradation by the proteasome pathway [20]. ROS generation activates ASK1 through the oxidation of an ASK1 inhibitor, thioredoxin [26]. Although pyrrolidinium fullerene and its derivatives induce ROS generation, this does not contribute to the activation of ASK1 and its downstream signals (Fig. 4). Yu et al. reported that JAK2 controls the expression level of ASK1 by directly phosphorylating ASK1 at tyrosine 718 [27]. However, we observed that the expression level of ASK1 was not affected by the expression of JAK2 V617F mutant, suggesting that JAK2-mediated stabilization of ASK1 seems to depend on the cell type.

The cellular inhibitor of apoptosis protein 1 (c-IAP1) was identified as the E3 ubiquitin ligase for ASK1 in the TNF α signaling pathway [28]. Although the detailed mechanism of how pyrrolidinium fullerene induces the degradation of ASK1 is unclear, pyrrolidinium fullerene and its derivatives may prompt the proteasomal degradation of ASK1 through ubiquitination by c-IAP1. Identification of the target protein of pyrrolidinium fullerenes will be a very important issue in future studies of pyrrolidinium fullerenes as anti-tumor drugs.

Supplementary data to this article can be found online at <http://dx.doi.org/10.1016/j.intimp.2014.02.035>.

Acknowledgments

We thank Dr. J. N. Ihle for the retroviral vectors of JAK2 and EpoR. This work was supported in part by grants (23790096, 21590072) from MEXT, Takeda Science Foundation, the Uehara Memorial Foundation and Keio Gijuku Fukuzawa Memorial Fund for the Advancement of Education and Research. This work was also supported by the Platform for Drug Discovery, Informatics, and Structural Life Science from the Ministry of Education, Culture, Sports, Science and Technology, Japan (25460073).

References

- [1] James C, Ugo V, Le Couédic JP, Staerk J, Delhommeau F, Lacout C, et al. A unique clonal JAK2 mutation leading to constitutive signalling causes polycythaemia vera. *Nature* 2005;434(7037):1144–8.
- [2] Kralovics R, Passamonti F, Buser AS, Teo SS, Tiedt R, Passweg JR, et al. A gain-of-function mutation of JAK2 in myeloproliferative disorders. *N Engl J Med* 2005;352(17):1779–90.
- [3] Levine RL, Wadleigh M, Cools J, Ebert BL, Wernig G, Huntly BJ, et al. Activating mutation in the tyrosine kinase JAK2 in polycythemia vera, essential thrombocythemia, and myeloid metaplasia with myelofibrosis. *Cancer Cell* 2005;7(4):387–97.
- [4] Funakoshi-Tago M, Pelletier S, Moritake H, Parganas E, Ihle JN. Jak2 FERM domain interaction with the erythropoietin receptor regulates Jak2 kinase activity. *Mol Cell Biol* 2008;28(5):1792–801.
- [5] Abe M, Funakoshi-Tago M, Tago K, Kamishimoto J, Aizu-Yokota E, Sonoda Y, et al. The polycythemia vera-associated Jak2 V617F mutant induces tumorigenesis in nude mice. *Int Immunopharmacol* 2009;9(7–8):870–7.
- [6] Funakoshi-Tago M, Tago K, Abe M, Sonoda Y, Kasahara T. STAT5 activation is critical for the transformation mediated by myeloproliferative disorder-associated JAK2 V617F mutant. *J Biol Chem* 2010;285(8):5296–307.
- [7] Kamishimoto J, Tago K, Kasahara T, Funakoshi-Tago M. Akt activation through the phosphorylation of erythropoietin receptor at tyrosine 479 is required for myeloproliferative disorder-associated JAK2 V617F mutant-induced cellular transformation. *Cell Signal* 2011;23(5):849–56.
- [8] Plo I, Nakatake M, Malivert L, de Villartay JP, Giraudier S, Villeval JL, et al. JAK2 stimulates homologous recombination and genetic instability: potential implication in the heterogeneity of myeloproliferative disorders. *Blood* 2008;112(4):1402–12.
- [9] Sumi K, Tago K, Kasahara T, Funakoshi-Tago M. Aurora kinase A critically contributes to the resistance to anti-cancer drug cisplatin in JAK2 V617F mutant-induced transformed cells. *FEBS Lett* 2011;585(12):1884–90.
- [10] Nakatake M, Monte-Mor B, Debili N, Casadevall N, Ribrag V, Solary E, et al. JAK2(V617F) negatively regulates p53 stabilization by enhancing MDM2 via La expression in myeloproliferative neoplasms. *Oncogene* 2012;31(10):1323–33.
- [11] Ueda F, Sumi K, Tago K, Kasahara T, Funakoshi-Tago M. Critical role of FANCC in JAK2 V617F mutant-induced resistance to DNA cross-linking drugs. *Cell Signal* 2013;25(11):2115–24.
- [12] Kroto H, Heath JR, O'Brien SC, Curl RF, Smalley RE. *Nature* 1995;318:162–3.
- [13] Kroto H, Space, stars, c60, and soot. *Science* 1988;242(4882):1139–45.
- [14] Mashino T, Shimotohno K, Ikegami N, Nishikawa D, Okuda K, Takahashi K, et al. Human immunodeficiency virus-reverse transcriptase inhibition and hepatitis C virus RNA-dependent RNA polymerase inhibition activities of fullerene derivatives. *Bioorg Med Chem Lett* 2005;15(4):1107–9.
- [15] Nakamura S, Mashino T. Water-soluble fullerene derivatives for drug discovery. *J Nippon Med Sch* 2012;79(4):248–54.
- [16] Mashino T, Usui N, Okuda K, Hirota T, Mochizuki M. Respiratory chain inhibition by fullerene derivatives: hydrogen peroxide production caused by fullerene derivatives and a respiratory chain system. *Bioorg Med Chem* 2003;11(7):1433–8.
- [17] Mashino T, Nishikawa D, Takahashi K, Usui N, Yamori T, Seki M, et al. Antibacterial and antiproliferative activity of cationic fullerene derivatives. *Bioorg Med Chem Lett* 2003;13(24):4395–7.
- [18] Shoji M, Takahashi E, Hatakeyama D, Iwai Y, Morita Y, Shirayama R, et al. Anti-influenza activity of c60 fullerene derivatives. *PLoS One* 2013;8(6):e66337.
- [19] Nishizawa C, Hashimoto N, Yokoo S, Funakoshi-Tago M, Kasahara T, Takahashi K, et al. Pyrrolidinium-type fullerene derivative-induced apoptosis by the generation of reactive oxygen species in HL-60 cells. *Free Radic Res* 2009;43(12):1240–7.
- [20] Funakoshi-Tago M, Nagata T, Tago K, Tsukada M, Tanaka K, Nakamura S, et al. Fullerene derivative prevents cellular transformation induced by JAK2 V617F mutant through inhibiting c-Jun N-terminal kinase pathway. *Cell Signal* 2012;24(11):2024–34.
- [21] Ichijo H, Nishida E, Irie K, ten Dijke P, Saitoh M, Moriguchi T, et al. Induction of apoptosis by ASK1, a mammalian MAPKKK that activates SAPK/JNK and p38 signaling pathways. *Science* 1997;275(5296):90–4.
- [22] Wang C, Mayer JA, Mazumdar A, Fertuck K, Kim H, Brown M, et al. Estrogen induces c-myc gene expression via an upstream enhancer activated by the estrogen receptor and the AP-1 transcription factor. *Mol Endocrinol* 2011;25(9):1527–38.
- [23] Iavarone C, Catania A, Marinissen MJ, Visconti R, Acunzo M, Tarantino C, et al. The platelet-derived growth factor controls c-myc expression through a JNK- and AP-1-dependent signaling pathway. *J Biol Chem* 2003;278(50):50024–30.
- [24] Funakoshi-Tago M, Sumi K, Kasahara T, Tago K. Critical roles of Myc-ODC axis in the cellular transformation induced by myeloproliferative neoplasm-associated JAK2 V617F mutant. *PLoS One* 2013;8(1):e52844.
- [25] Deng H, Zhang J, Yoon T, Song D, Li D, Lin A. Phosphorylation of Bcl-associated death protein (Bad) by erythropoietin-activated c-Jun N-terminal protein kinase 1 contributes to survival of erythropoietin-dependent cells. *Int J Biochem Cell Biol* 2011;43(3):409–15.
- [26] Liu H, Nishitoh H, Ichijo H, Kyriakis JM. Activation of apoptosis signal-regulating kinase 1 (ASK1) by tumor necrosis factor receptor-associated factor 2 requires prior dissociation of the ASK1 inhibitor thioredoxin. *Mol Cell Biol* 2000;20(6):2198–208.
- [27] Yu L, Min W, He Y, Qin L, Zhang H, Bennett AM, et al. JAK2 and SHP2 reciprocally regulate tyrosine phosphorylation and stability of proapoptotic protein ASK1. *J Biol Chem* 2009;284(20):13481–8.
- [28] Zhao Y, Conze DB, Hanover JA, Ashwell JD. Tumor necrosis factor receptor 2 signaling induces selective c-IAP1-dependent ASK1 ubiquitination and terminates mitogen-activated protein kinase signaling. *J Biol Chem* 2007;282(11):7777–82.

HETEROCYCLES, Vol. 90, No. 2, 2015, pp. 1168 - 1178. © 2015 The Japan Institute of Heterocyclic Chemistry
Received, 28th July, 2014, Accepted, 28th August, 2014, Published online, 11th September, 2014
DOI: 10.3987/COM-14-S(K)92

SYNTHESIS OF PYRROLIDINOFULLERENES VIA SINGLE ELECTRON TRANSFER REACTION OF ARYLDIENAMINES WITH C₆₀

Naohiko Ikuma,* Hiroyuki Yamamoto, Ken Kokubo, Takumi Oshima

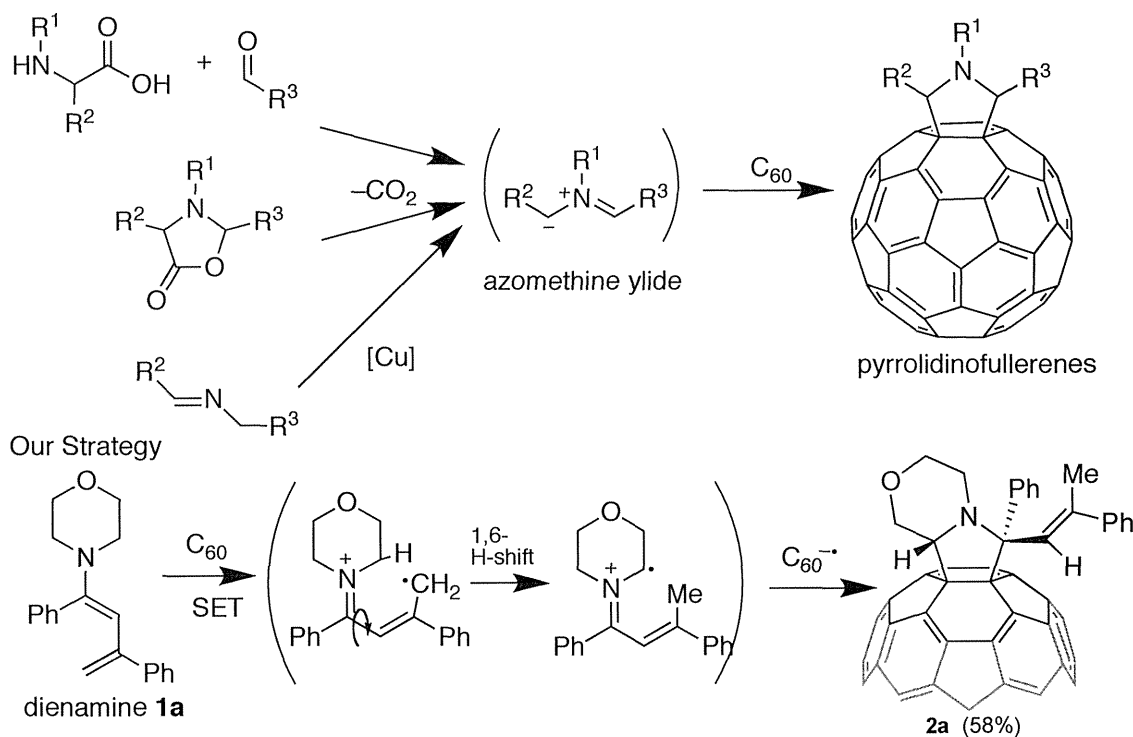
Division of Applied Chemistry, Graduate School of Engineering, Osaka University, Osaka 565-0871, Japan

E-mail: ikuma@chem.eng.osaka-u.ac.jp

Abstract – Various aryl-substituted pyrrolidinofullerenes were synthesized via a single electron transfer (SET) reaction of diaryldienamines with C₆₀ and the following consecutive 1,6-hydrogen shift and the [3 + 2] cycloaddition of the generated radical ion pair. The LUMO levels of pyrrolidinofullerenes were ca. 0.1 eV higher than C₆₀, consequently suppressing the bisadduct formation. The phenyl-substituted pyrrolidinofullerene **2a** representatively exhibited the protic acid-catalyzed intramolecular Friedel–Crafts cyclization and the DDQ induced oxidative reversion into C₆₀.

INTRODUCTION

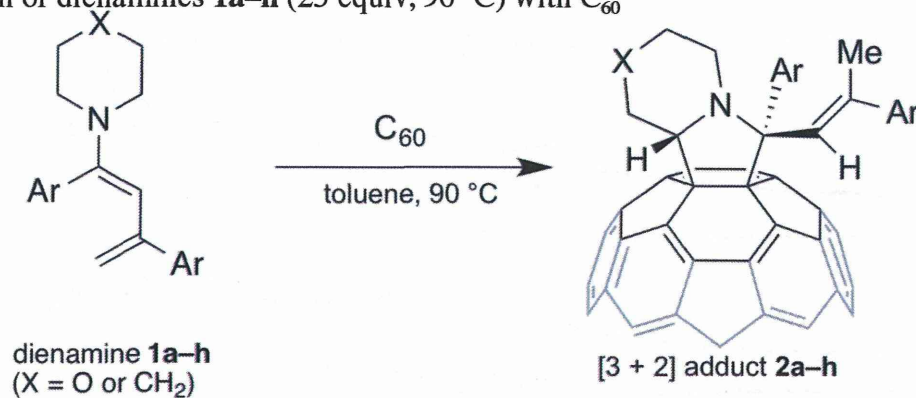
Pyrrolidinofullerenes^{1–6} are useful fullerene derivatives in materials chemistry and for medicinal applications, as liquid crystals,⁵ light-converting substances,⁶ and chiral fullerene compounds.^{3,4} These fullerenes are easily synthesized from the [3 + 2] cycloaddition of azomethine ylides which were prepared from various precursors such as carbonyl compound/amino acid (Prato reaction),^{1,2} aziridine,^{1,3} lactone,¹ and imine.⁴ In very recent communication, we have reported that morpholinodiphenyldienamine **1a** underwent a single electron transfer (SET) reaction with C₆₀ to give diarylpyrrolidinofullerene **2a** via the subsequent 1,6-hydrogen shift and the [3 + 2] cycloaddition of the radical cation with C₆₀ radical anion (Scheme 1).⁷ We also confirmed the reaction mechanism by DFT calculations as well as the radical-trapping experiment. In this paper, we report the synthesis of variously aryl-substituted pyrrolidinofullerenes by way of this SET/H-shift process. Moreover, we have examined the electronic properties and thermal stability (by DSC and TGA), TfOH catalyzed transformation, and DDQ induced oxidative degradation.



Scheme 1

RESULTS AND DISCUSSION

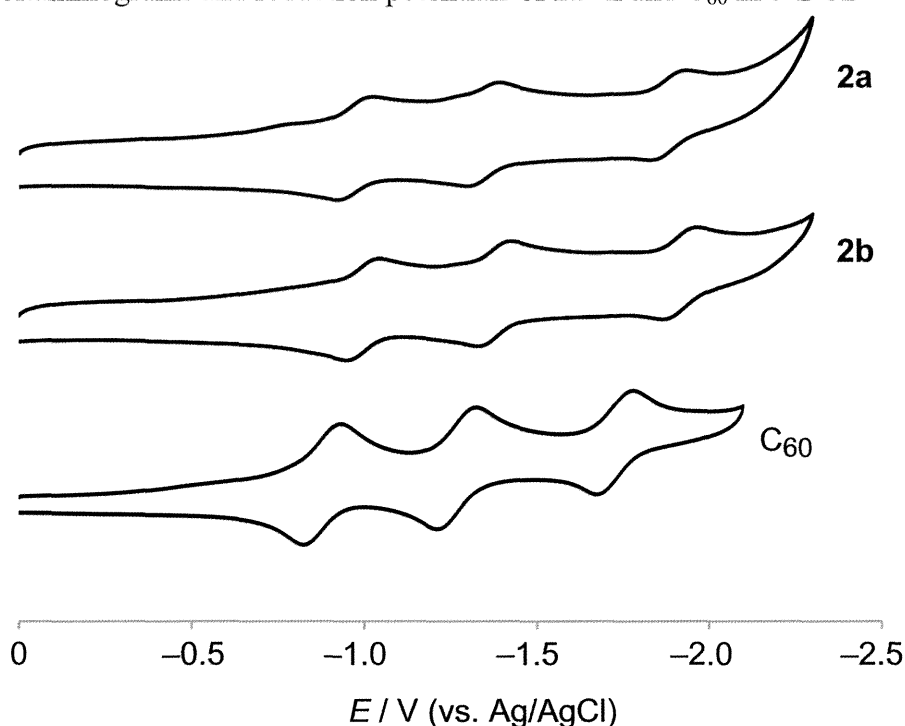
As in the case of **2a**, variously aryl-substituted pyrrolidinofullerenes **2b–h** were synthesized as shown in Table 1. Dienamines **1b–h** were prepared by the condensation of arylketones and cyclic amines with *p*-toluenesulfonic acid (TsOH) catalyst. Due to the lability, less volatile dienamines **1b–h** were immediately used for the reaction with C_{60} without further purification and identification. These crude dienamines (ca. 25 equiv) were reacted with C_{60} in toluene at 90 °C. The reaction was traced by HPLC (Buckyprep column, toluene eluent). Unfavorable contaminants such as enamines and unreacted arylketones appreciably neither inhibited the present cycloaddition nor brought about the side reactions. The reaction solution was evaporated and the residue was submitted for column chromatography to give pure monoadducts **2b–h** in slightly lower yields (ca. 20–40 %) than **2a**. Piperidinodienamine **1b** reacted faster than morpholinodienamine **1a** on account of higher electron-donating piperidine substituent, so that the isolated yield of **2b** slightly decreased due to the formation of multiadducts. Similarly, the reaction of morpholinodienamines with donative aryl groups such as 4-alkylphenyl (**1d–f**) and thiophene **1h** gave slightly lower yields because of the multiaddition. On the other hand, *p*-chlorophenyl-substituted dienamine **1c** needed slightly longer reaction time because of lower electron-donating ability. The $^1\text{H}/^{13}\text{C}$ NMR spectra of these 1:1 adducts showed similar signals to those of **2a**; appearances of methyl group and asymmetric morpholino/piperidino ring were only explained by the hydrogen shift of dienamino radical cation and [3 + 2] cycloaddition.

Table 1. Reaction of dienamines **1a–h** (25 equiv, 90 °C) with C₆₀

	Amine	Ar	Time (h)	Conv. (%) ^b	Yield (%) ^c
1a^a			17	89	58
1b			3.5	92	33
1c			20	87	42
1d			14	88	30
1e			15	88	29
1f			16	90	24
1g			16	90	42
1h			17	83	21

^aFrom the preliminary communication.⁷ ^bDetermined by HPLC area ratio. ^cIsolated yields.

For the application to electronic materials, we estimated the electron affinity of pyrrolidino-fullerenes **2a–h**. Cyclic voltammogram measurements showed ca. 0.1 V lower reduction potentials than that of C₆₀, implying the pyrrolidino-fusion lowered the electrophilicity of fullerene core (Table 2). This lowering electron affinity of monoadducts will suppress further SET reaction giving bisadducts. However, these substituent effects are not so effective because of indirect inductive effect of the aryl substituents.

Table 2. Cyclic voltammograms and reduction potentials of **2a–h** and C₆₀ in *o*-DCB^a

Compd	$E^{1/2}V$ vs Fc/Fc ⁺		
	$E_{1\text{red}}$ (LUMO level/eV) ^b	$E_{2\text{red}}$	$E_{3\text{red}}$
2a	-1.17 (-3.63)	-1.55	-2.08
2b	-1.20 (-3.60)	-1.58	-2.12
2c	-1.16 (-3.64)	-1.54	-2.07
2d	-1.18 (-3.62)	-1.56	-2.10
2e	-1.14 (-3.66)	-1.53	-2.06
2f	-1.15 (-3.65)	-1.53	-2.08
2g	-1.15 (-3.65)	-1.55	-2.11
2h	-1.16 (-3.64)	-1.55	-2.09
C ₆₀	-1.08 (-3.72)	-1.46	-1.91

^aElectrolyte 0.1 M TBAP; scan rate 100 mV s⁻¹; potentials measured vs Ag/Ag⁺ reference electrode and standardized to Fc/Fc⁺ couple [$E_{\text{Fc/Fc}^+} = +0.203$ V vs Ag/Ag⁺ (*o*-DCB)]. ^bValues from the vacuum level were estimated using the following equation; LUMO level = $-(E_{1\text{red}}^{1/2} + 4.8)$.⁸

Thermal stability of **2a** was evaluated by DSC (Figure 1a) and TGA (Figure 1b) measurements. One endothermic peak followed by exothermic plateau in DSC and drastic weight loss (ca. 13%) in TGA were observed around 260–270 °C, suggesting melting with decomposition. This decomposition temperature is comparable with those of pyrrolidinofullerenes bearing BOC-group (>250 °C),^{6b} but lower than those of liquid pyrrolidinofullerenes with stable alkoxyphenyl groups (340–420 °C).⁹ These previous studies indicate the pyrrolidino ring seems to be stable around 300 °C unless the compound has less stable substituents such as BOC group. Thus we can consider the decomposition of **2a** at 265 °C is due to the

elimination of methylstyrene moiety, in consistent with the weight loss of TGA (F.W. of CH=CMePh is 117, whereas M.W. of **2a** is 1012).¹⁰

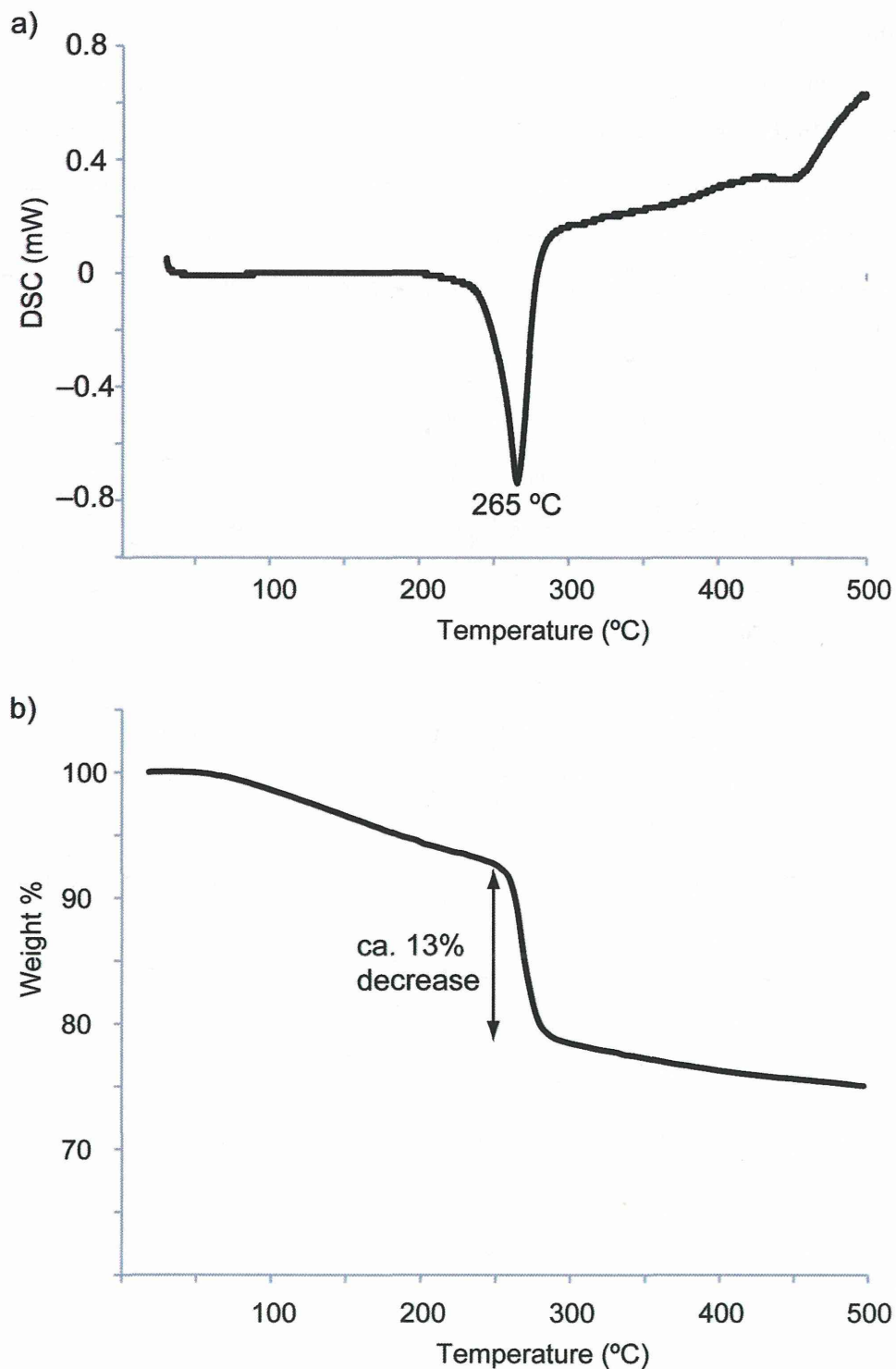
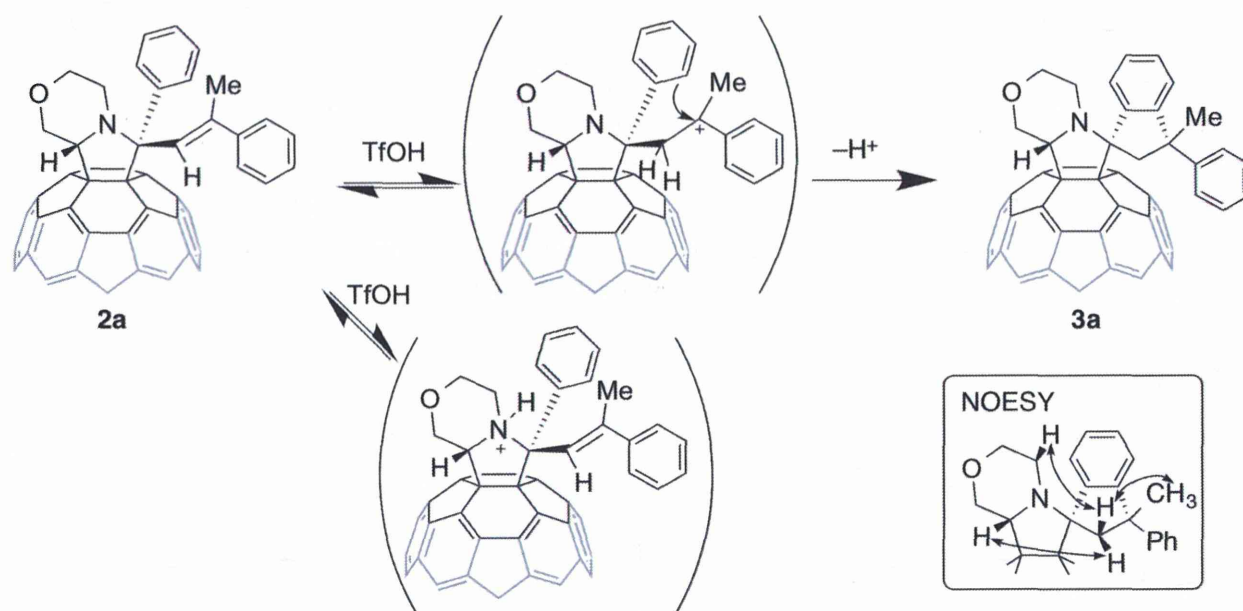


Figure 2. a) DSC and b) TGA measurements of **2a** under N₂ atmosphere.

We have carried out acid treatment of **2a** because these pyrrolidinofullerenes inherently have basic site at the nitrogen of pyrrolidino moiety. However, by adding excess amount of TfOH (25 equiv), the amino linkage was retained but the intramolecular Friedel–Crafts type cyclization occurred to give spiro

compound **3a** (Scheme 2) as confirmed by $^1\text{H}/^{13}\text{C}$ NMR and 2D-HSQC/HMBC/NOESY correlation (Supporting Information). Similar to styrene which easily polymerizes with electrophilic initiator, phenylvinyl group of **2a** may be protonated at the β -position to form relatively stable benzylic carbocation. This cationic center is attacked by adjoining phenyl ring to construct the stable dihydroindene ring.¹¹ In this acid treatment, although pyrrolidino function can be protonated, the resulting quarterly ammonium ion seems to persist any further transformation. The reaction proceeded in various polar aromatic solvents such as *o*-DCB, and anisole (Table 3). Anisole and toluene provided slightly lower yield, probably because these solvents are likely to participate in the Friedel–Crafts reaction at the fullerene sphere.^{12,13}



Scheme 2

Table 3. Reaction of **2a** with TfOH (25 equiv) in various solvents

Solvent	Temp (°C)	Time (h)	Conversion (%) ^a	Yield of 3a (%) ^b
benzene	80	3	98	40
toluene	80	4	95	27
chlorobenzene	80	5	95	59
anisole	80	5	90	28
<i>o</i> -DCB	80	5	90	56
DMF	80	24	-	-
chloroform	80	24	20	5

^a Determined by HPLC area ratio. ^b Isolated yields.

Pyrrolidinofullerenes are known to undergo the cycloreversion into azomethine ylide and C_{60} under the influence of oxidant such as Cu(II) and trapping dipolarophiles.¹⁴ Similarly, oxidation of **2a** by DDQ led to the regeneration of C_{60} even without trapping agents (Scheme 3). Since the unsubstituted